ICSV14
Cairns • Australia
9-12 July, 2007

14th International Congress on Sound & Vibration

FREQUENCY-DOMAIN PREDICTION OF SOUND PROPAGATION THROUGH AXISYMMETRIC FLOW DUCTS

X. D. Li[1], X.Y. Li[1] and F. Thiele[2]

[1]School of Jet Propulsion, Beihang University (BUAA)
Beijing 100083, P.R. China
[2]Institute of Fluid Mechanics and Engineering Acoustics
Berlin University of Technology, D10623 Berlin, Germany
lixd@buaa.edu.cn

Abstract

A frequency-domain approach for computational aeroacoustics is developed for the prediction of azimuthal sound modes propagating in axisymmetric flow ducts. Different pseudo-time marching methods are implemented and compared including an upwind scheme, a four-stage Runge-Kutta scheme and a dual-time scheme. Numerical validation for hard walled ducts including simple and complex geometries are presented to evaluate the accuracy and efficiency of the proposed methods. It is shown that all the implemented time marching methods can achieve converged numerical solutions. Comparatively, the four-stage Runge-Kutta scheme is most efficient, while the upwind scheme is the most time consuming. The local time stepping technique can accelerate numerical computation to some extent. The dual-time scheme has the advantage of improving the numerical accuracy and expanding the numerical stability range.

1. INTRODUCTION

The prediction of acoustic propagating through complex nacelle geometry with lining treatment and non-uniform mean flow is a key technology in the reduction of sound radiation from ducted fans. Various theoretical and computational methods have been developed for duct acoustics, such as the finite element, boundary element, multiple scale and computational aeroacoustics (CAA) methods. Comparatively, CAA methods have received much attention due to its capability for flow ducts with complex geometries. However, acoustic optimisation always requires very efficient numerical prediction tools in each run. Therefore, it is very important and desirable to develop very fast and accurate CAA methods for duct acoustics.
During the past ten years, both the time-domain and frequency-domain CAA methods have been developed for the simulation of sound propagating through lined flow ducts. For example, Li el al. [1] developed a time-domain CAA approach suitable for azimuthal sound mode propagating in axisymmetric flow ducts. Lan and Guo [2] developed a frequency-domain CAA method for axisymmetric lined flow ducts. Comparatively, time-domain CAA methods are more suitable for broadband, transient and nonlinear acoustic problems. Its main difficulty is on the construction of time-domain impedance boundary conditions. Frequency-domain methods

are more favourable for single frequency problems due to their efficiency. The pseudo-time marching methods that have been implemented and tested in previous frequency-domain CAA methods [2][3] are very limited, however. This paper aims to develop efficient and accurate frequency-domain CAA approaches for axisymmetric flow ducts through comparing different pseudo-time stepping methods.
The paper is organized as follows. Section 2 presents the governing equations and numerical algorithms. In section 3, numerical validation and testing results are provided and analysed for circular ducts and aero-engine intake geometries. A conclusion is given in section 4.

2. GOVERNING EQUATIONS AND NUMERICAL ALGORITHEM

2.1 Governing equation

The governing equations are the 2.5-D Euler equation linearized about a mean flow in the frequency-domain.

$$i\omega\tilde{Q} + A\frac{\partial\tilde{Q}}{\partial x} + B\frac{\partial\tilde{Q}}{\partial r} + \frac{1}{r}C\tilde{Q} + D\tilde{Q} = 0 \tag{1}$$

where, $$A = \begin{pmatrix} u_0 & \gamma p_0 & 0 & 0 \\ \frac{1}{\rho_0} & u_0 & 0 & 0 \\ 0 & 0 & u_0 & 0 \\ 0 & 0 & 0 & u_0 \end{pmatrix}, \quad B = \begin{pmatrix} v_0 & 0 & \gamma p_0 & 0 \\ 0 & v_0 & 0 & 0 \\ \frac{1}{\rho_0} & 0 & v_0 & 0 \\ 0 & 0 & 0 & v_0 \end{pmatrix},$$

$$C = \begin{pmatrix} \gamma v_0 & 0 & \gamma p_0 & im\gamma p_0 \\ 0 & 0 & 0 & 0 \\ 0 & 0 & 0 & 0 \\ \frac{im}{\rho_0} & 0 & 0 & v_0 \end{pmatrix}, \quad D = \begin{pmatrix} \gamma(\frac{\partial v_0}{\partial r} + \frac{\partial u_0}{\partial x}) & \frac{\partial p_0}{\partial x} & \frac{\partial p_0}{\partial r} & 0 \\ -\frac{\frac{\partial p_0}{\partial x}}{\gamma\rho_0 p_0} & \frac{\partial u_0}{\partial x} & \frac{\partial u_0}{\partial r} & 0 \\ -\frac{\frac{\partial p_0}{\partial r}}{\gamma\rho_0 p_0} & \frac{\partial v_0}{\partial x} & \frac{\partial v_0}{\partial r} & 0 \\ 0 & 0 & 0 & 0 \end{pmatrix},$$

$$\tilde{Q} = (\rho, u, v, w, p)^T$$

where x and r are the axial and radical coordinates, respectively. The mean variables ρ_0, p_0, u_0, v_0 represent the mean flow density, pressure and velocity components, respectively. The variables ρ, p, u, v, w represent the complex perturbations of density, pressure, and velocity components, respectively. m denotes the circumferential mode number; i is the imaginary number; ω is the angular frequency, γ is the ratio of the specific heats.
Eq. (1) can be written into the following form:

$$i\omega\tilde{Q} = F(\tilde{Q}) \tag{2}$$

2.2 Numerical algorithms

Through the introduction of pseudo-time marching technique, Eq. (2) can be formulated as:

$$\frac{\partial\tilde{Q}}{\partial t} = F\left(\tilde{Q}\right) - i\omega\tilde{Q} \tag{3}$$

where t is introduced as the pseudo time.

Different time-marching methods can be used to discretize Eq. (3). The first order implicit upwind time marching method is the most straightforward one which can be expressed as:

$$\frac{\tilde{Q}^{n+1} - \tilde{Q}^{n}}{\Delta t} = -i\omega\tilde{Q}^{n+1} + F(\tilde{Q}_n) \tag{4}$$

where the superscript n denotes the pseudo-time level $n\Delta t$.
This method was used in the frequency-domain method of Lan and Guo [2].
The second pseudo-time disretization method for Eq. (3) is the four-stage Runge-Kutta time integration scheme [5] written in the folllowing form:

$$\begin{aligned}
&\tilde{Q}^{(0)} = \tilde{Q}^{(n)},\\
&\tilde{Q}^{(1)} = \tilde{Q}^{(0)} - \alpha_1\Delta t[\bar{F}(\tilde{Q}^{(0)})],\\
&\tilde{Q}^{(2)} = \tilde{Q}^{(0)} - \alpha_2\Delta t[\bar{F}(\tilde{Q}^{(1)})],\\
&\tilde{Q}^{(3)} = \tilde{Q}^{(0)} - \alpha_3\Delta t[\bar{F}(\tilde{Q}^{(2)})],\\
&\tilde{Q}^{(4)} = \tilde{Q}^{(0)} - \alpha_4\Delta t[\bar{F}(\tilde{Q}^{(3)})],\\
&\tilde{Q}^{(n+1)} = \tilde{Q}^{(4)}
\end{aligned} \tag{5}$$

where $\bar{F} = F(\tilde{Q}) - i\omega\tilde{Q} + D$, α_i is the coefficient of the Runge-Kutta scheme $(i = 1,2,3,4)$, and D is the damping term.
Özyörük and Alpman [3] implemented this scheme in their frequency-domain method. To accelerate solution convergence, a local time stepping technique [4] is implemented and tested. Furthermore, a dual time stepping technique [6] is implemented through coupling the four-stage Runge-Kutta (RK) scheme and the first order implicit upwind scheme. Introducing a fictitious time τ, Eq. (3) can be reformulated as

$$\frac{\partial\tilde{Q}}{\partial\tau} = \frac{\partial\tilde{Q}}{\partial t} + F\left(\tilde{Q}\right) - i\omega\tilde{Q} = \hat{F}(\tilde{Q}) \tag{6}$$

where a new residual, $\hat{F}(\tilde{Q})$, is introduced containing the derivative of time t. By introducing the derivative of time τ, the system of Eq. (6) is advanced in time using an explicit four-stage RK scheme to realize the subiterative process, which can be written as:

$$
\begin{aligned}
&\tilde{Q}^{(0)} = \tilde{Q}^{(n)}, \\
&\tilde{Q}^{(1)} = \tilde{Q}^{(0)} - \alpha_1 \Delta\tau [F^*(\tilde{Q}^{(0)})], \\
&\tilde{Q}^{(2)} = \tilde{Q}^{(0)} - \alpha_2 \Delta\tau [F^*(\tilde{Q}^{(1)})], \\
&\tilde{Q}^{(3)} = \tilde{Q}^{(0)} - \alpha_3 \Delta\tau [F^*(\tilde{Q}^{(2)})], \\
&\tilde{Q}^{(4)} = \tilde{Q}^{(0)} - \alpha_4 \Delta\tau [F^*(\tilde{Q}^{(3)})], \\
&\tilde{Q}^{(n+1)} = \tilde{Q}^{(4)}
\end{aligned}
\tag{7}
$$

where the initial value $\tilde{Q}^{(n)}$ is derived from the outer iterative loop, D denotes the damping term, $F^* = \hat{F} + D$.
The Dispersion-Relation-Preserving scheme (DRP)[7] is implemented for spatial discretization Appropriate boundary conditions are implemented for inflow, outflow and wall boundaries. Detailed information about the numerical approach can be found in our previous time-domain CAA method [1].

3. NUMERICAL RESULTS AND ANALYSIS

Two straight circular ducts subjected to a subsonic uniform mean flow/without flow are firstly selected for validation and evaluation of developed frequency domain method. Then the sound propagation through an aero-engine intake is numerically simulated for checking the accuracy and feasibility for complex geometries.

3.2 Sound propagation in straight circular ducts

In the first circular duct case, a uniform grid with $\Delta x = \Delta r = 0.01$ is distributed in the interior domain along both the x and r directions. The total number of grid points used in the computation is 127×54 including a stretched buffer zone. The grid resolution is 12.5 PPW along the x direction in the interior domain. The sound source is excited against the uniform mean flow of $M_0 = -0.5$ for $m = 10$, $n = 1$, $\omega = 12$. Fig.1 shows the outer wall pressure distribution compared between the numerical solution of upwind scheme and the analytical solution. Fig.2 shows the outer wall pressure distribution compared between the numerical solution of RK scheme and the analytical solution. Both of the numerical solutions agree well with the analytical solutions. It can be noticed that the numerical solution by RK scheme agrees better than the results by the upwind scheme.

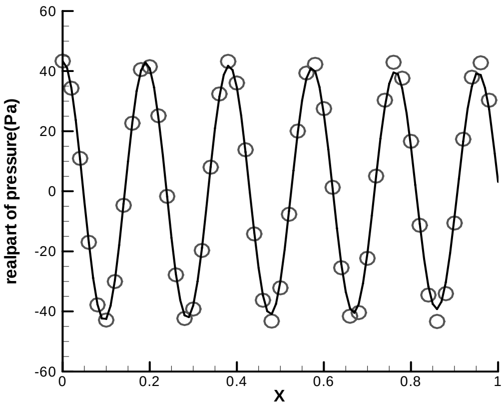

Figure 1. Upwind: analytical(○), numerical(—)

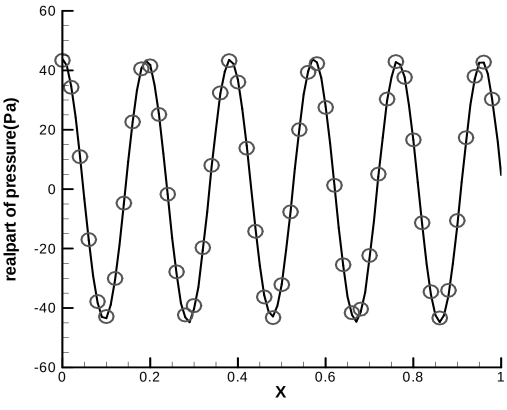

Figure 2. RK: analytical(○) ,numerical(—)

In the second circular duct case, a uniform grid with $\Delta x = \Delta r = 0.02$ is distributed in the interior domain along both the x and r directions. The total number of grid points used in the computation is 209×54 including a stretched buffer zone. The grid resolution is 14 PPW along the x direction in the interior domain. Numerical computations are performed on an Intel(R) Pentium(R) 4/1.60GHz processor for the case of $M_0 = 0$, $m = 10, n = 1$, $\omega = 24$. Fig. 3 shows the outer wall pressure distribution compared between the numerical solution of upwind scheme and the dual-time step scheme. Fig. 4 shows the outer wall pressure distribution compared between the numerical solution of Runge-Kutta scheme and the local-time step scheme. All the numerical results by different time stepping methods agree very well.

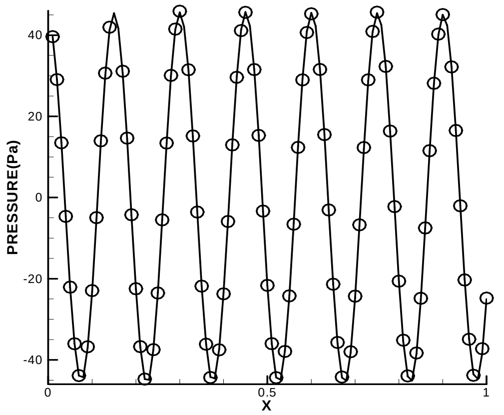

Figure 3. Upwind(○),dual time stepping(—)

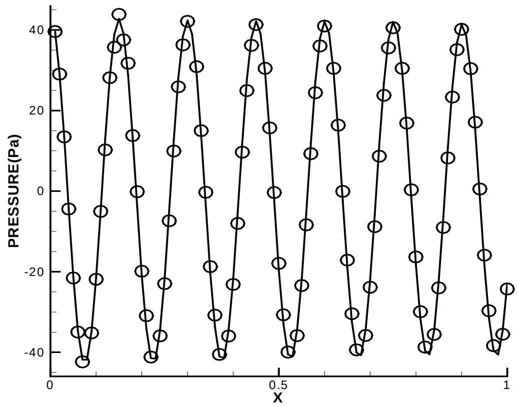

Figure 4. RK(○),local time stepping(—)

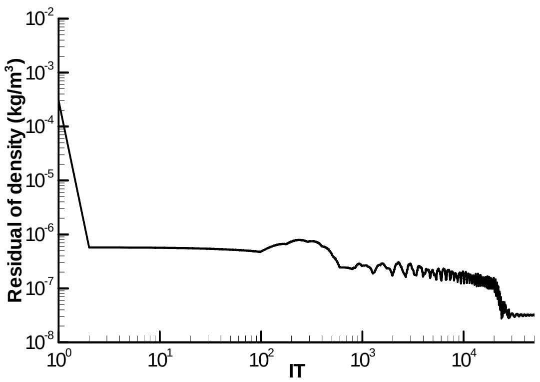

Figure 5. Convergence history: upwind scheme

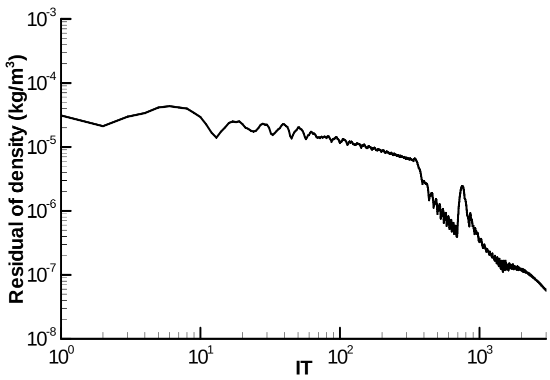

Figure 6. Convergence history: RK scheme

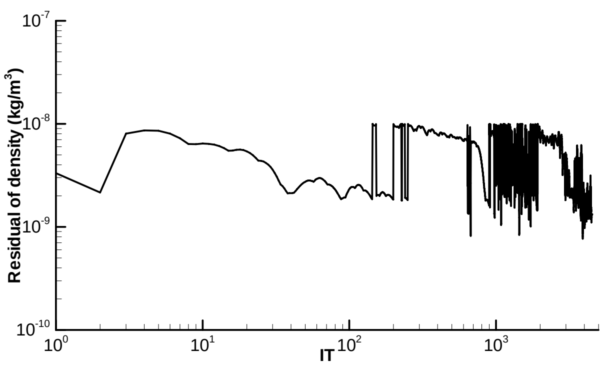

Figure 7. Convergence history: dual time stepping

Fig.5-7 show the convergence histories by upwind, RK, and dual time stepping method, respectively. The magnitude of density perturbation is around 10^{-4}kg/m^3. The residual of the density reach a good converged solution in the range of 10^{-7}~10^{-9} for each scheme. Table 1 presents the comparison of the total CPU time, iteration steps and residual accuracy by three different schemes. It is clear that the RK scheme is the most efficient method whereas the dual-time stepping is the most accurate method.

Table 1. Comparison between different time stepping schemes

Schemes	Total CPU time (s)	Iteration steps	Accuracy (kg/m^3)
Upwind	42500	50000	10^{-7}
RK	720	2000	10^{-7}
Dual time stepping	3200	5000	10^{-9}

3.2 Sound propagation through an aero-engine intake

In this case, an aero-engine intake from Rienstra and Eversman [8] is selected for validation. A 651×151 body fitted gird is generated for numerical computations. The ducted fan case is run on a cluster of Intel(R) Pentium(R) 4/3.00G processors. A total of two processors were used for this case. The Runge-Kutta scheme and the dual-time stepping scheme are utilized to compute the sound propagating through the duct intake for the case of $M_0 = -0.5, m = 10, n = 1, \omega = 16$. Fig.8 and Fig.9 show the convergence histories by the RK scheme and the RK scheme with the local time stepping technology, respectively. The RK scheme with local time stepping technology requires 2000-2500 steps to obtain converged numerical solutions while 3000-5000 steps will be required by the explicit RK scheme without local time stepping technology. The time step size is given by the CFL number of 1.2 by the RK scheme and 0.9 by the RK scheme with the local time stepping technology implemented, respectively. The residual of the density by the RK scheme can reach a good converged solution with an accuracy of 10^{-7} while the RK scheme with the local time stepping technique can reach a convergence solution in the accuracy of 10^{-6}. Fig.10. shows the convergence history: by the dual time stepping which requires 40000-50000 steps to reach a convergence solution with an accuracy of 10^{-9}.

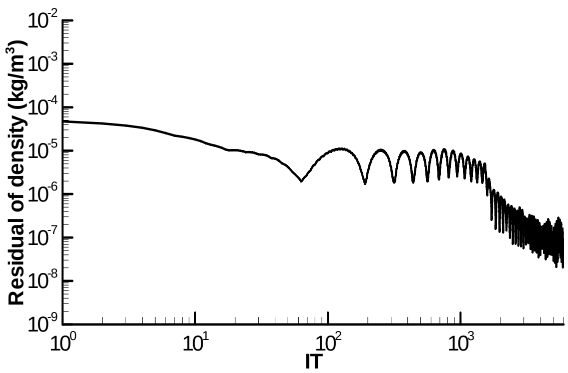

Figure 8. Convergence history: RK

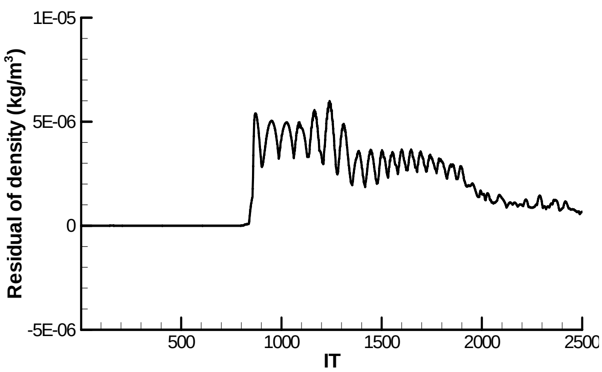

Figure 9. Convergence history: local time stepping

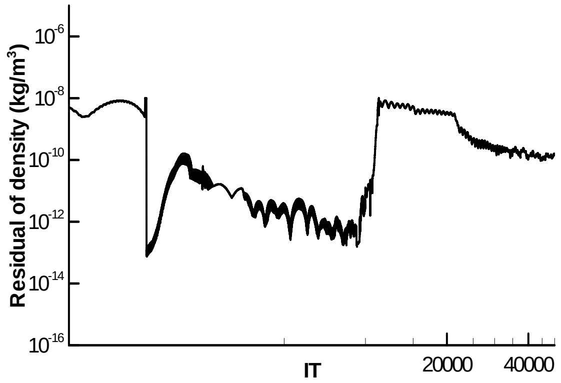

Figure 10. Convergence history: dual time stepping

The normalized pressure contours are shown in Fig.11 and Fig. 12 .The contours in Fig.11 was calculated by the Runge-Kutta method and in Fig. 12, by the local time stepping method. It can be observed that the numerical result by the RK method is slightly smoother than the result from the scheme with the local time stepping in the region near the axis. Fig.13 shows the normalized pressure contours by the dual time stepping scheme, which gives the smoothest solution of these three methods. For further comparison, Fig.14 gives the time-domain CAA results from Li, et al. [1]. There is a good agreement between the frequency domain results and the time domain results.

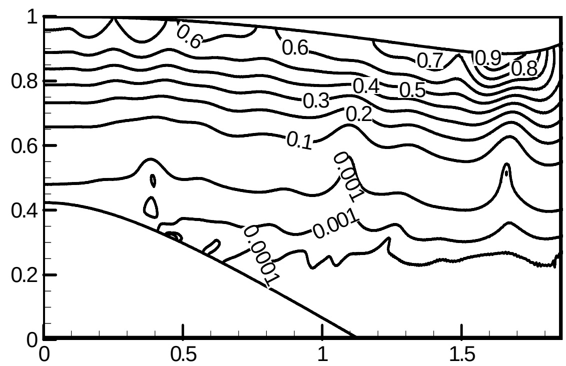

Figure 11. Normalized pressure contours
(RK in frequency domain)

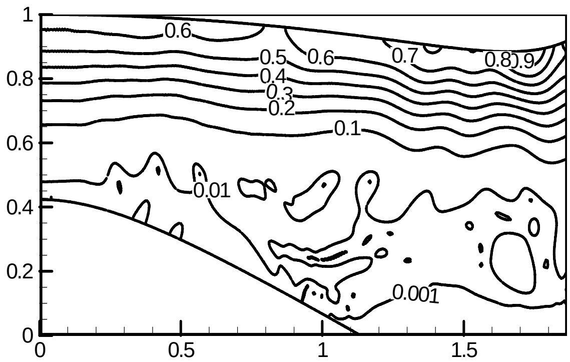

Figure 12. Normalized pressure contours
(RK with local time stepping in frequency domain)

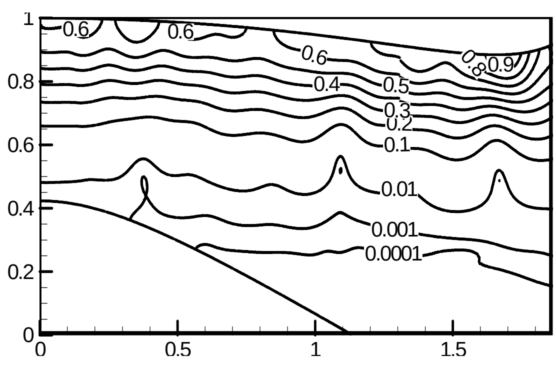

Figure13. Normalized pressure contours
(Dual time stepping in frequency domain)

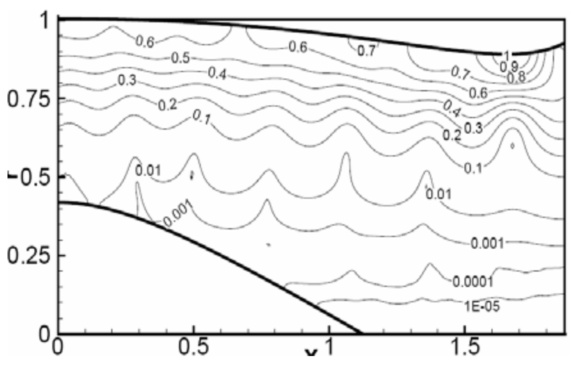

Figure 14. Normalized pressure contours
(CAA in time domain)

4. CONCLUSIONS

A frequency-domain CAA approach is developed for the prediction of sound propagation through axisymmetric flow ducts. Several pseudo-time discretization methods are implemented, validated and evaluated. Numerical results show that the explicit Runge-Kutta scheme with the local time stepping technique can lead to the fastest convergence of the numerical solution. Although the dual-time stepping method can't achieve the same convergence rate as the Runge-Kutta scheme, it can improve numerical accuracy and expand numerical stability range.

ACKNOWLEDGEMENT

This work is supported by grants from the NSFC-50676003, ASFC-05C51030 and the 111 project B07009 of China.

REFERENCES

[1] X. D. Li, C. Schemel, U. Michel, and F. Thiele, "Azimuthal Sound Mode Propagation in Axisymmetric Flow Ducts", *AIAA Journal*, Vol.l42, No.10, October 2004, pp.2019-2027.

[2] J.H. Lan and Y.P. Guo, "Validation of Acoustic Propagation Code with JT 15D Static and Flight Test Data", *AIAA Paper*, 2004-2986, 2004.

[3] Y.Özyörük, E.Alpman, V.Ahuja, L.N.Long, "Frequency-domain prediction of turbofan noise radiation", *Journal of Sound and Vibration*, Vol. 270, 2004, pp.933-950.

[4] M. S. McMullen, "The application of non-linear frequency domain methods to the Euler and Navier-Stokes equations", *Ph.D. Dissertation, Stanford* University, March 2003.

[5] A. Jameson, Schmidt and E. Turkel, "Numerical Solution of the Euler Equations by Finite Volume Methods Using Rung-Kutta Time-Stepping Schemes", *AIAA paper,* 1981-1259, 1981.

[6] A. Jameson, "Time Dependent Calculations Using Multigrid with Applications to Unsteady Flows Past Airfoils and Wings", *AIAA Pape*r 91-1596, 1991.

[7] C.K.W. Tam and J.C. Webb, "Dispersion-Relation-Preserving Difference Scheme for Computational Acoustics", *Journal of Computational Physics*, Vol.107, 1993, pp.262-281.

[8] S.W. Rienstra and W. Eversman, "A Numerical Comparison Between the Multiple-Scale and Finite-Element Solution for Sound Propagation in Lined Flow Ducts," *Journal of Fluid Mechanics*, Vol. 437, June 2001, pp. 367–384.